Electronic Supplementary Material (ESI) for Lab on a Chip.

Deterministic droplet-based co-encapsulation and pairing of microparticles via active sorting and downstream merging

Meng Ting Chung[a], Daniel Núñez[b], Dawen Cai[b,c*], Katsuo Kurabayashi[a,d*]

[a] Department of Mechanical Engineering, University of Michigan, Ann Arbor, MI, 48105, USA

[b] Department of Cell & Developmental Biology, University of Michigan, Ann Arbor, MI, 48105,USA

[c] Department of Biophysics, College of LS&A, University of Michigan, Ann Arbor, MI, 48105, USA

[d] Department of Electrical Engineering and Computer Sci., University of Michigan., Ann Arbor, MI, 48105, USA

[*]To whom correspondence should be addressed. E-mail: dwcai@umich.edu and katsuo@umich.edu

Supporting material

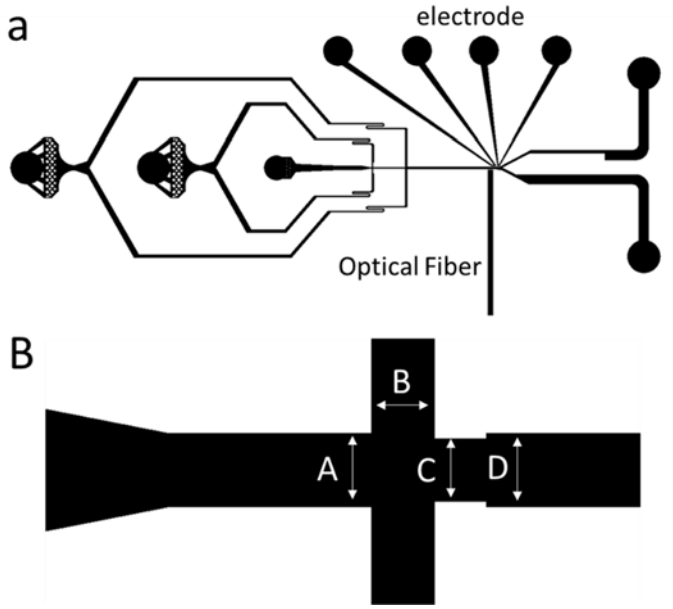

Fig. S1 (a) CAD layout of droplet generating/sorting device (top view). (b) Dimensions of flow-focusing zone. For generating larger (80 μm) droplets: B=C=60 μm, A=D=70 μm, channel height=70 μm. For smaller (40 μm) droplets: A=B=30 μm, C=25 μm, D=40 μm, channel height=45 μm.

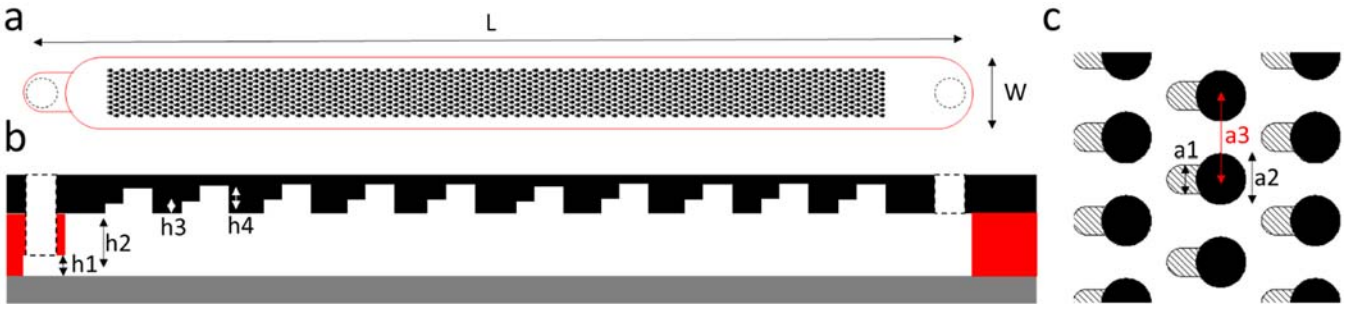

Fig S2 Design of droplet merging device. (a) Top view of the whole device. The red line represents the microfluidic channel structure and the black patterns represent the array of microwells. L=25mm, w=2mm. Array size = 9 rows × 128 columns =1,152 microwells (b) Side view of the device (the drawing is not to scale). h_1=100 μm, h_2=500 μm, h_3=40 μm, h_4=70 μm. (c) The lattice structure of the array. a_1=45μm, a_2=80 μm, a_3=140 μm.

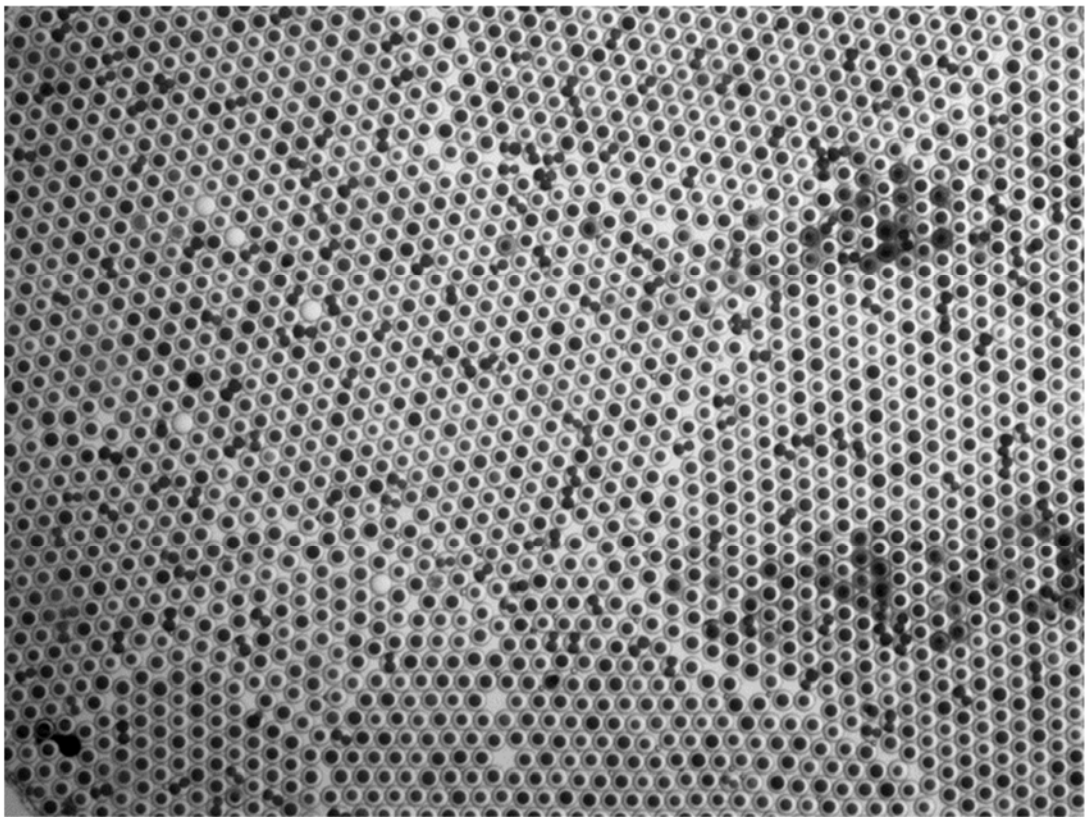

Fig. S3 The images show the droplets generated from our droplet generating/sorting devices. 80μm-diameter droplets contain TOYOPEARL microbeads. About 99.5% of droplets encapsulate one or more than one beads.

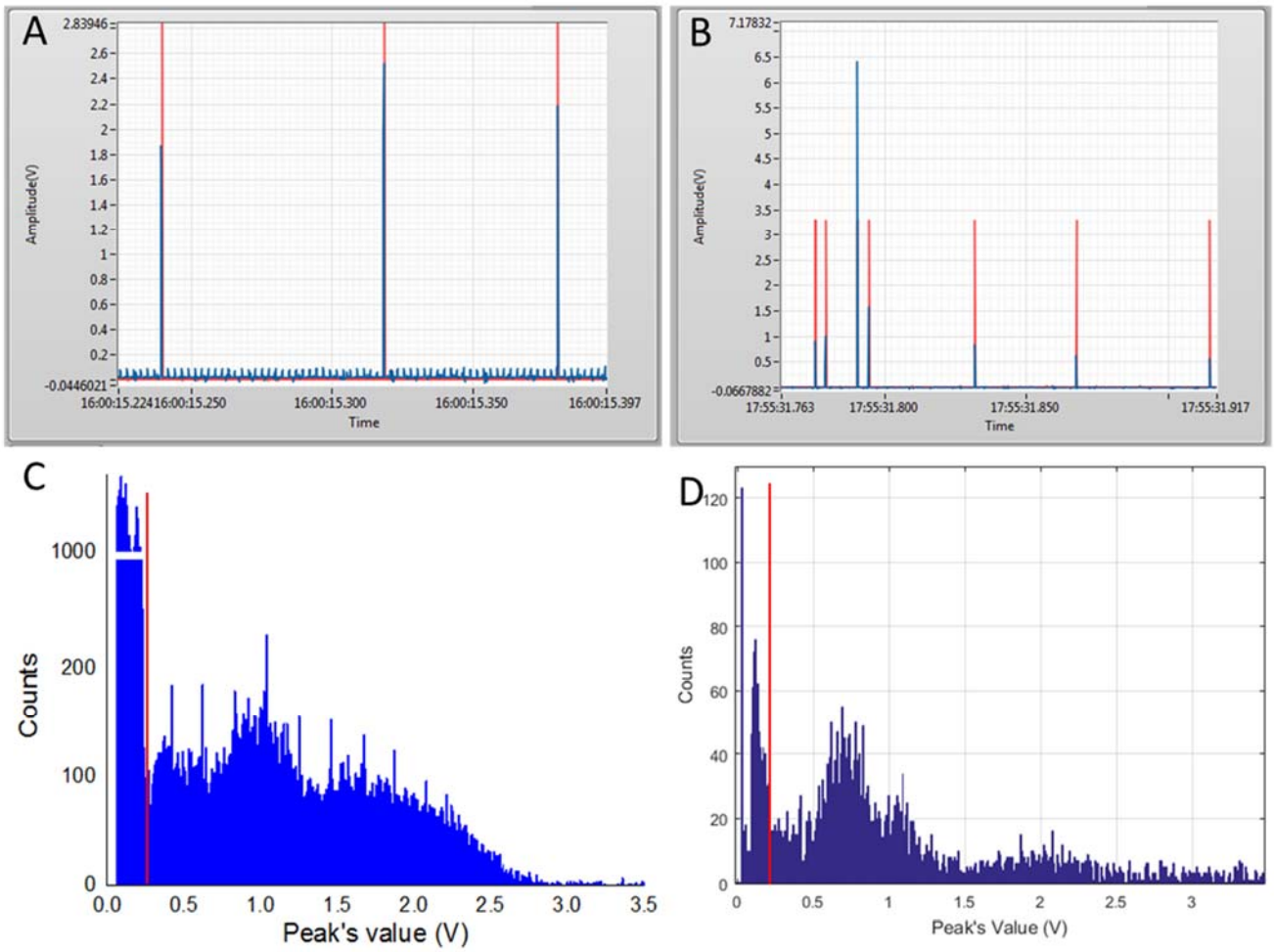

Fig. S4 (A)Time sequence of scattering light signals (blue line) detected from empty droplets (peak value ~0.1V) and droplets encapsulating 30μm non-fluorescent beads (type-a). The red line indicates the TTL signal which triggers the sorting events. The *x*-axis represents system clock readings (hours: minutes: seconds. milliseconds). (B) Fluorescence signals detected from droplets encapsulating 15μm fluorescent beads (type-b). The empty droplets contain no fluorescent molecules, therefore, cannot be detected. (C,D) Histograms of detected peak values for type-*a* (C) and type-*b* (D) beads extracted from (A) and (B) The red line indicates the sorting gate value.

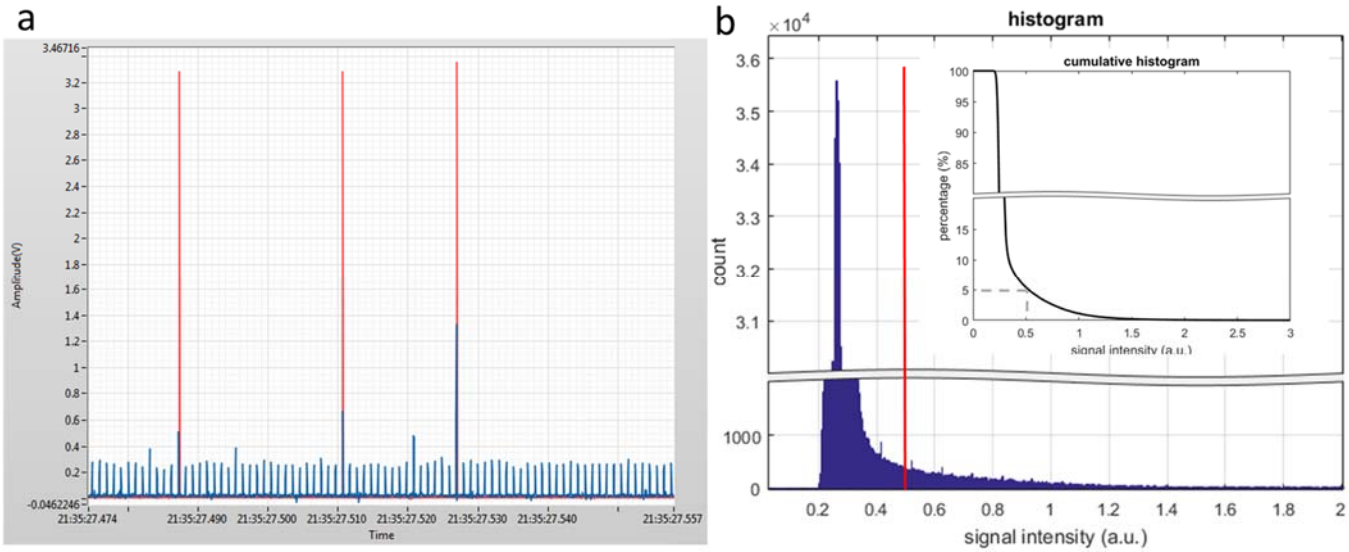

Fig. S5 (a) Time sequence of scattering light signals (blue line) detected from empty droplets (peak value ~0.3V) and droplets with Hela cells. The red line indicates the TTL signal which triggers the sorting. The *x*-axis represents system clock readings (hours: minutes: seconds. milliseconds). (b) Histograms of detected peak values extracted from (a) for Hela cell-encapsulating droplets. The red line indicates the sorting gate value which is set be the top 5% among all peaks' intensity.

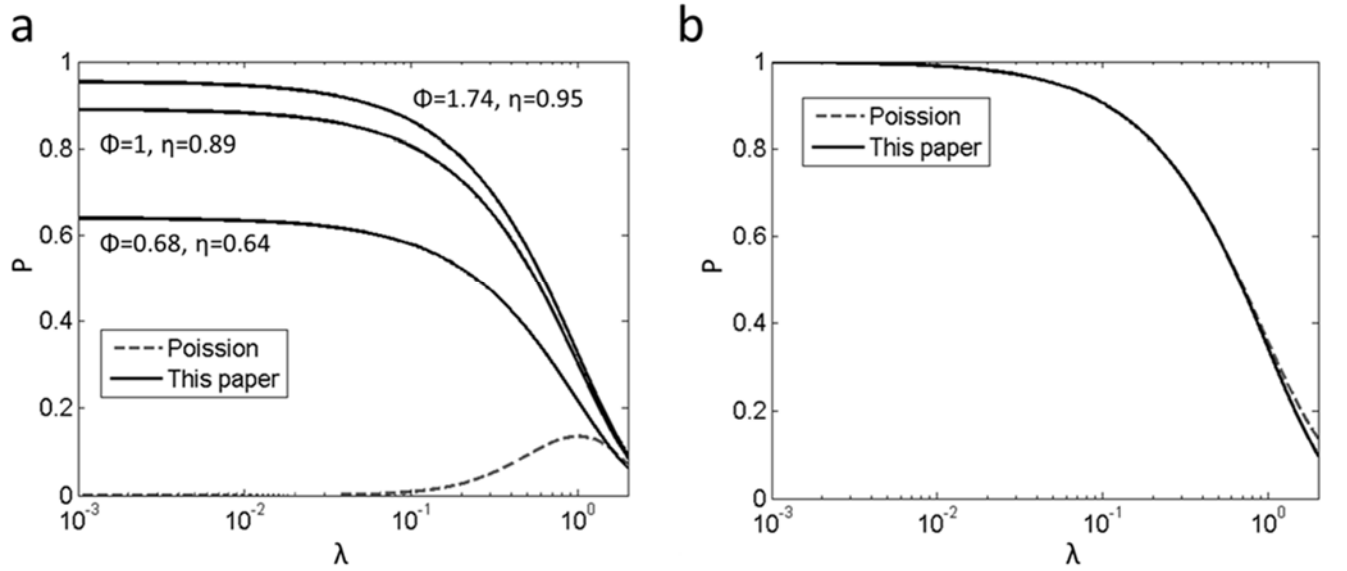

Fig. S6 (a) Predicted probability of producing droplets that exactly encapsulate a one-to-one type-*a*/type-*b* particle pair ($k_a = k_b = 1$) as a function of the initial particle concentration λ. For simplicity, it is assumed that the two types of particles have the same concentration ($\lambda_a = \lambda_b = \lambda$). The solid lines indicate the results of our approach, predicted by equation (2) in the main text ($\Phi =$

$\frac{Number\ of\ input\ 40\mu m\ droplets}{1152\ (size\ of\ merging\ array)}$, η= occupancy of the 40μm droplets). The dashed line indicates the result predicted by the *Poisson* statistics. (b) Predicted fraction of a one-to-one pair of type-*a* and type-*b* particles ($k_a = k_b = 1$) encapsulated within a droplet to a particle combination satisfying the condition of $\{k_a, k_b \in N | k_a + k_b \geq 2 \cap k_a, k_b \neq 0\}$ within the same droplet as function of the initial particle concentration λ. This figure represents the accuracy predicted for some type of single-cell assays, eg. Drop-seq.

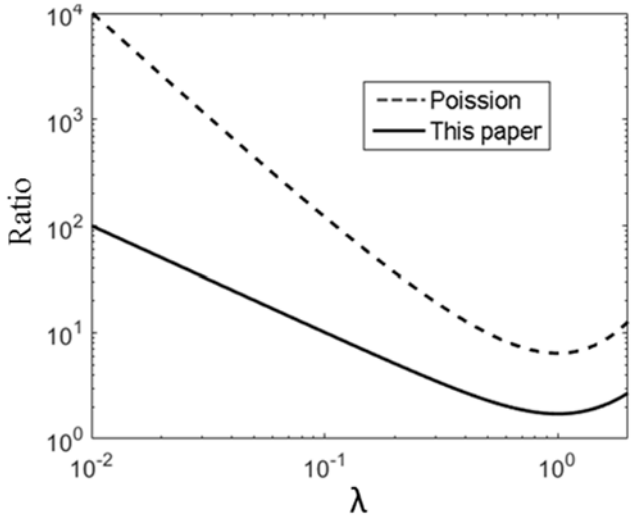

Fig. S7 Predicted volume ratio of waste droplets to droplets encapsulating one-to-one particle pairs as a function of the initial particle concentration λ. This figure indicates the 1-2 orders of magnitude higher reagent cost effectiveness of our assay as compared to the conventional assay following the *Poission* statistics.